Proceedings of the ASME Summer Conference on Heat Transfer
HT2008
August 10-14, 2008, Jacksonville, Florida, USA

HT2008-56233

Slip-flow and Conjugate Heat Transfer in Rectangular Microchannels

H.D. Madhawa Hettiarachchi **Mihajlo Golubovic**

William M. Worek **W.J. Minkowycz**

Department of Mechanical and Industrial Engineering

University of Illinois at Chicago

842 W Taylor Street, Chicago IL 60607

ABSTRACT

Slip-flow and conjugate heat transfer in rectangular microchannels are studied numerically for thermally developing laminar flow subjected to constant wall temperature (T) and constant wall heat flux (H2) boundary conditions. A three-dimensional numerical code based on finite volume method is developed to solve the coupled energy equations in the wall and fluid regions together with temperature jump at the wall-fluid boundary. A modified convection-diffusion coefficient at the wall-fluid interface is defined to incorporate the temperature-jump boundary condition. The numerical code is validated by comparing the present results with the published data. The effect of rarefaction and wall conduction on the heat transfer in the entrance region is analyzed in detail. Results show that the wall conduction has a considerable influence on the developing Nusselt number along the channel for the H2 boundary condition, particularly at low Knudsen numbers. In the case of the T thermal boundary condition, negligible influence of wall conduction on the Nusselt number is observed for all Knudsen numbers considered.

INTRODUCTION

Traditional examples of fluids in slip-flow include low pressure fluidic flow systems such as those occurring in vacuum and aerospace engineering devices [1]. Recent advances in micro-nano fabrication technologies and development of microscale thermal fluidic systems have opened a new area where the dynamics of slip-flow is applicable [2].

One of the major difficulties predicting the fluid flow and heat transfer in micro-nano sized channels can be attributed to the rarefaction effects that occur in the fluids when the channel dimensions become comparable to the mean free path of the fluid molecules. These circumstances result in non-continuum regions in the fluid that will influence the velocity profile, pressure drop and heat transfer in the channels. The Knudsen number is a measure of the degree of the rarefaction which is defined as the ratio of mean free path to the characteristic length scale of the system. For small Knudsen numbers, $Kn \le 10^{-3}$, the fluid is considered to be a continuum, while for large values, $Kn \ge 10$, free molecular flow is assumed. The slip-flow region studied here is in the range of $10^{-3} \le Kn \le 10^{-1}$, where molecular collisions with the walls dominate over intermolecular collisions resulting in a breakdown of the continuum assumption in a thin layer adjacent to the walls called the Knudsen layer. It is well established that for the slip flow regime, the standard Navier-Stokes equations can still be used with modified boundary conditions for slip velocity at the walls [2]. Ebert and Sparrow [3] have studied slip flow in rectangular channels and provided a correlation for the slip flow profile as a function of Kn and aspect ratio (α).

The extended Graetz problem with velocity slip and temperature jump at the wall has been studied analytically for constant wall temperature and heat flux boundary conditions by several researchers [4-6]. Axial conduction effects were neglected in all solutions and the simplified energy equation is solved analytically for hydrodynamically fully developed flow. Steady-state two-dimensional heat transfer in microtubes was studied numerically for different boundary conditions by Sun et al.[7]. Biswal et al. [8] studied numerically 2D slip-flow in a vertical channel including the influence of gravity. Dongari et al. [9] investigated the application of second-order slip model to solve two-dimensional fully developed slip-flow in long microchannels. Slip-flow heat transfer in rectangular micro channels has been studied by several researches [10-14]. Yu et al. [10, 11] studied laminar slip-flow heat transfer in microchannels for thermally developing flow subjected to constant wall temperature and isoflux boundary conditions. The energy equation was solved analytically using an integral transform technique neglecting axial conduction. Hadjiconstantinou [12] investigated the constant wall temperature convective heat transfer characteristics for gaseous flow in a two-dimensional microchannel under hydrodynamically and thermally fully-developed conditions. It was shown that for the slip flow region, the continuum approach predictions are in good agreement with the Direct Simulation Monte Carlo (DSMC) results. Renksizbulut et al. [13] solved slip flow and heat transfer in the entrance region of rectangular microchannels for cases where the Prandtl number is equal to unity. Hettiarachchi et al. [14] studied the slip flow and heat transfer in rectangular microchannels with constant temperature walls for range of parameters considering simultaneously and thermally developing flow conditions. It was assumed that the temperature of the fluid at the surface is finitely different from the wall temperature due to breakdown of the continuum flow near the walls. The above studies show the importance of implementing the temperature jump boundary condition in solving the energy equation in the slip flow region. Neglecting this effect could lead to a significant over prediction of the heat transfer.

The entrance region of microchannels is particularly of interest due to the presence of large pressure drop and heat transfer, and the relative size. Also, the effect of axial conduction becomes important for low Pelcet numbers which is typical in microchannel flows. In this study, three-dimensional slip flow conjugate heat transfer in rectangular mirochannels is studied using a finite-volume method for T and H2 thermal boundary conditions. The axial conduction effect is included in the solution. The non-dimensionalized governing equations are solved using the SIMPLE method. Implementation of the temperature-jump and dicretization of the energy equation at the wall are explained. The effect of rarefaction and wall thermal conductivity on the heat transfer in the entrance region is analyzed for various values of *Kn* and conduction ratio (K_s/K_f), considering thermally developing flow with T and H2 boundary conditions.

NOMENCLATURE

A	Area
a	convection-diffusion parameter
c_p	specific heat
D_h	hydraulic diameter
D	non-dimensionalized wall thickness, defined as d/D_h
d	wall thickness
Ec	Eckert number
fRe	Friction relation
H	non-dimensionalized height of the microchannel, defined as h/D_h
h	height of the microchannel
k	thermal conductivity
Kn	Knudsen number
L	non-dimensionalized length of the microchannel, defined as l/D_h
l	length of the microchannel
Nu	Nusselt number
Pr	Prandtl number
Q”	non-dimensionalized heat flux
q''	heat flux
Re	Reynolds number
T	temperature
u	fluid velocity
U	non-dimensional fluid velocity
W	non-dimensionalized width of the microchannel, defined as w/D_h
w	width of the microchannel
X,Y,Z	non-dimensional coordinates, defined as x/D_h, y/D_h *and* z/D_h, respectively.
x,y,z	Cartesian coordinates
Z^+	nond-imensional axial length, $Z/(D_hRe)$
Z^*	reciprocal Graetz number, $Z/(D_hPrRe)$

Greek symbols

α	aspect ratio
β	parameter defined by Eq. (11)
γ	specific heat ratio
θ	nondimensionalized temperature
μ	viscosity
ρ	density
σ_T	thermal accommodation coefficient
σ_V	momentum accommodation coefficient
ϕ	eigenvalues defined by Eq. (8)
φ_i	dependent variables

Subscripts

ave	average
b	wall-fluid boundary
i,j	array indices
f	fluid
m	mean
nb	neighboring control volumes (*nb*=1...6)
w	wall
1,2,3,4,5,6	neighboring grid points

ANALYSIS

The structure of the microchannel and coordinate system considered in this analysis is shown in Fig. 1. The aspect ratio is given by $\alpha = H/W$ where H and W are the dimensionless height and width of the channel passage, respectively. A uniform dimensionless wall thickness, D, around the channel passage is considered. The flow is considered along the Z axis. The dimensionless channel length, *L*, is chosen so that the thermally developed flow is reached at the exit.

The numerical model for heat transfer in the microchannel was developed under the following assumptions.

1. Steady fluid flow and heat transfer

2. The flow is incompressible and laminar.

3. Constant wall and fluid properties.

4. Negligible radiation heat transfer.

5. Body forces and viscous dissipation are ignored.

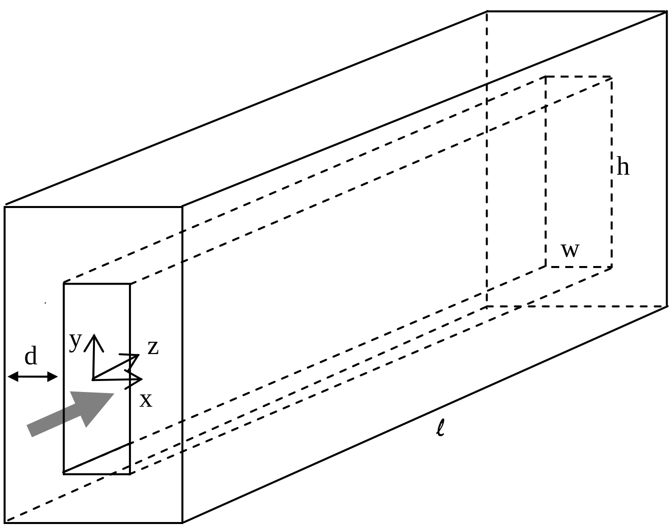

Fig. 1 Schematic diagram of the rectangular microchannel passage and surrounded wall.

Based on the above assumptions, the governing equations describing heat transfer in the microchannel can be written as follows.

The energy equation for the cooling fluid,

$$\rho c_p u_j \frac{\partial T_i}{\partial x_j} = k\nabla^2 T \quad , \tag{1}$$

and for the solid wall,

$$k_w \nabla^2 T \quad = 0 \, . \tag{2}$$

The energy equation is non-dimensionalized using following dimensionless parameters,

$$X_i = \frac{x_i}{D_h} \, , U_i = \frac{u_i}{u_{ave}} \, . \tag{3}$$

For the constant wall temperature (T) boundary case, the temperature is non-dimensionalized as,

$$\theta = \frac{T - T_{in}}{T_w - T_{in}} \, , \tag{4}$$

and for the constant heat flux (H2) boundary case, the temperature is non-dimensionalized as,

$$\theta = \frac{T - T_{in}}{q_w^{"} D_h \, / \, k_f} \, . \tag{5}$$

For both T and H2 thermal boundary cases, the non-dimensionalzed energy equation for the fluid flow becomes,

$$U_j \frac{\partial \theta}{\partial X_j} = \frac{1}{\text{RePr}} \nabla^2 \theta \quad , \tag{6}$$

and for the wall,

$$\frac{k_w}{k_f} \frac{1}{\text{RePr}} \nabla^2 \theta = 0 \quad . \tag{7}$$

The non-dimensional heat flux at the wall-fluid interface satisfies the energy conservation as,

$$Q_b^{"} = \left(\frac{\partial \theta}{\partial n} \right)_f = \frac{k_w}{k_f} \left(\frac{\partial \theta}{\partial n} \right)_w \, . \tag{8}$$

The local Nusselt number is determined as,

$$Nu_z = \frac{Q_b^{"}}{(\theta_{w,b} - \theta_{f,ave})} \, . \tag{9}$$

The non-dimensionalized constant wall boundary temperature, θ_w, and non-dimensionalized constant wall boundary heat flux become unity for cases of T and H2, respectively. At the channel inlet, a fully developed fluid velocity profile and uniform temperature ($\theta_{in} = 0$) are prescribed. At the exit, since fully-developed conditions are assumed, the *Z* direction velocity and temperature gradients are set to zero. A zero pressure is assigned at the flow exit while a zero pressure gradient is applied to all other boundaries including the inlet while temperature jump condition is satisfied at the walls.

Ebert and Sparrow [3] have presented an analytical solution for fully developed slip flow velocity profile in a rectangular channel. It could be presented according to the coordinate system and non-dimensional variables considered in this analysis as follows,

$$U(X,Y)=\frac{HW}{4A}\sum_{k=1}^{\infty}\left(\begin{array}{l}\frac{\cos\phi_k X}{\phi_k^3}\left(\frac{\sin(\phi_k H/2)}{(H/2+Kn\sin^2(\phi_k H/2))}\right)\cdot\\ \left(1-\frac{\cosh\phi_k Y}{\cosh\phi_k W/2+Kn\,\phi_k\sinh(\phi_k W/2)}\right)\end{array}\right), \tag{10}$$

where

$$A=\sum_{k=1}^{\infty}\phi_k^{-5}\left(\frac{\sin^2\phi_k H/2}{H/2+Kn\sin^2\phi_k H/2}\right)\left(\phi_k W/2-\frac{\tanh\phi_k W/2}{1+Kn\,\phi_k\tanh\phi_k W/2}\right). \tag{11}$$

ϕ_i values are evaluated using the eigen function,

$$\cot(\phi_i\ H/2)=\phi_i Kn\ . \tag{12}$$

In no-slip flow analysis, velocity and temperature continuity is enforced along all solid-fluid interfaces. In the slip flow region, a discontinuity of the velocity and temperature at the solid-fluid interface arises due to breakdown of the local thermodynamic equilibrium between the wall and the fluid adjacent to the wall.

The non-dimensinalized temperature jump at the solid-liquid interface is given as [2],

$$\theta_{jump}=-\frac{2-\sigma_T}{\sigma_T}\left(\frac{2\gamma}{\gamma+1}\right)\frac{Kn}{\Pr}\frac{\partial\theta}{\partial n}, \tag{13}$$

where, $\frac{\partial\theta}{\partial n}$ is the corresponding transverse temperature gradient in the fluid at the solid–fluid interface.

The thermal accommodation coefficient, σ_T, describe the interaction of the fluid molecules with the wall. Generally, its value depends on the surface finish, temperature and velocity at the fluid-solid interface, and is determined experimentally. It varies from near zero to unity for specular and fully-diffused reflections, respectively. For most engineering applications, the thermal accommodation coefficient is near unity and considering approximate nature of the slip flow, it is taken as unity in this study.

The non-dimensional form of the simplified temperature-jump boundary condition can be expressed as,

$$\theta_{jump}=-\frac{Kn}{\beta}\frac{\partial\theta}{\partial n}, \tag{14}$$

where, $$\beta=\left(\frac{\gamma+1}{2\gamma}\right)\Pr\ . \tag{15}$$

The parameter β is a function of Prandtl number (Pr) and specific heat ratio (γ) of the fluid.

NUMERICAL SOLUTION

Due to the symmetry, a quarter of the channel is considered in the analysis. A non-uniform grid arrangement is used in all X,Y and Z directions. A large number of grid points are used near the channel inlet and channel inner walls to resolve the developing flow region and large velocity and thermal gradients.

The numerical solution is obtained by discretizing the governing equations using the finite-volume method as described by Patankar [15]. The Power-law scheme is used to interpolate the convection-diffusion coefficients at the faces of control volumes. The resulting set of algebraic equations in X,Y, and Z directions are solved using line-by-line method. The solution is assumed to be convergent when the all dependent variables, φ, are satisfied the condition, $\left|(\varphi^{n+1}-\varphi^{n})/\varphi^{n+1}\right|\le 10^{-6}$.

IMPLEMENTATION OF TEMPERATURE-JUMP BOUNDARY CONDITION AT THE WALL-FLUID INTERFACE

The discretizied energy equation for a control volume can be written as [15],

$$\sum_{nb=1}^{6}a_{nb}(\theta_{nb}-\theta_P)=b\ . \tag{16}$$

The coefficients a_{nb} present the convection and diffusion influence at the six neighboring faces and can be expressed in dimensionless terms as,

$$a_{nb}=D_{nb}A\left|P_{nb}\right|+Max\left[(-1)^{nb}F_{nb},0\right], \tag{17}$$

where

$$F_{nb}=(UA)_{nb},\ D_{nb}=\frac{1}{\mathrm{Re}\Pr k_f}\left(\frac{kA}{\delta X}\right)_{nb},\ P_{nb}=\frac{F_{nb}}{D_{nb}} \tag{18}$$

and $A|P_{nb}|$ was evaluated using power-low scheme.

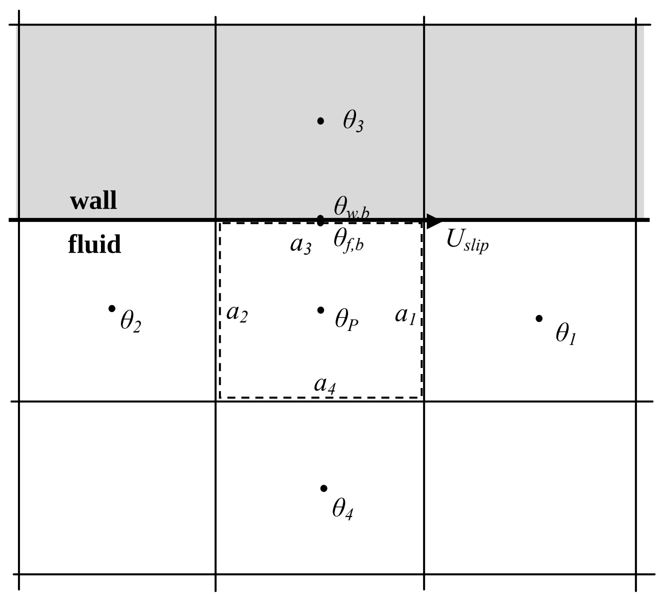

Fig. 2 Control volume adjacent to the wall (only two dimensions are shown for the simplicity).

The presence of a temperature-jump at the fluid-wall interface produces an additional thermal resistance to heat transfer across the interface. This effect should be taken into account in the discretized energy equations involving the fluid-wall interface.

A control volume adjacent to the wall-fluid interface is shown in Fig. 2. Temperature jump at the wall-fluid interface can be expressed as,

$$\theta_{jump} = \theta_{w,b} - \theta_{f,b} = -\frac{Kn}{\beta}\frac{\partial \theta}{\partial n}, \qquad (19)$$

where $\theta_{w,b}$ is the surface temperature of the wall and $\theta_{f,b}$ is the adjacent fluid temperature, which could be assumed infinitesimal distance apart. Using the thermal resistance concept, heat flow across the wall-fluid interface can be expressed in terms of temperature differences and the respective convection–diffusion coefficients as,

$$a_3(\theta_3-\theta_p) = a_{w,b}(\theta_3-\theta_{w,b}) = a_{f,b}(\theta_{f,b}-\theta_p) = a_{slip}(\theta_{w,b}-\theta_{f,b}), \qquad (20)$$

and the overall convection-diffusion coefficient across the wall-fluid interface, a_3, can be expressed as,

$$\frac{1}{a_3} = \frac{1}{a_{w,b}} + \frac{1}{a_{f,b}} + \frac{1}{a_{slip}}. \qquad (21)$$

$a_{b,w}$ and $a_{b,f}$ can be determined by considering the no-slip flow condition as,

$$\frac{1}{a_{3,no-slip}} = \frac{1}{a_{w,b}} + \frac{1}{a_{f,b}}. \qquad (22)$$

Thus, the overall convection-diffusion coefficient across the wall-fluid interface, a_3, can be expressed in terms of the no-slip flow convection-diffusion coefficient, $a_{3,no-slip}$ and the additional heat transfer coefficient resulting from the temperature jump, a_{slip}, as,

$$\frac{1}{a_3} = \frac{1}{a_{3,no-slip}} + \frac{1}{a_{slip}}. \qquad (23)$$

Using Eq. (19), the heat flow across the wall-fluid interface can be written as,

$$a_{slip}\theta_{jump} = -\frac{A}{\mathrm{Re}\,\mathrm{Pr}}\frac{\partial \theta}{\partial n} = \frac{\beta}{Kn}\frac{A}{\mathrm{Re}\,\mathrm{Pr}}\theta_{jump}, \qquad (24)$$

and the heat transfer coefficient resulting from the temperature jump, a_{slip}, can be determined as,

$$a_{slip} = \frac{\beta}{Kn}\frac{A}{\mathrm{Re}\,\mathrm{Pr}}. \qquad (25)$$

Therefore, dicretized equations for boundary control volumes can be written similar to internal control volumes with a modified convection-diffusion coefficient at the boundary, a_3, as given by equation (23).

GRID INDEPENDENCE AND VALIDATION

A non-uniform grid is considered in the *X*,*Y* and *Z* directions with a fine grid near the channel walls and in the entrance region where large gradients exist. The grid independence of the results was carried out by using different mesh sizes, and it was found that any grid size beyond 16x16x200 for the passage combined with 6x6x200 for the wall (with a stretching ratio of 4:4:100 in *X*,*Y* and *Z* directions, respectively) yield grid independent results. As aspect ratio increases, the size of the grid is adjusted to maintain grid independency.

The local Nusselt number along the microchannel axis is compared with the analytical solutions presented by Yu and Ameel [10, 11] for T and H2 cases with thermally developing flow and considering negligible fluid axial conduction. A very good agreement was observed between the present calculation and the Yu and Ameel [10, 11] solutions at different Knudsen numbers as shown in Fig.3. Further present results agree well with the no-slip flow data by Wilbulswas [16].

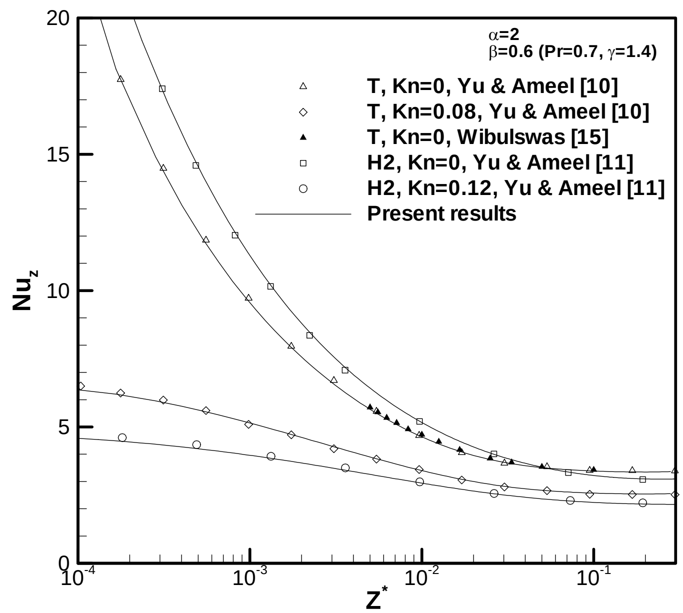

Fig. 3 Comparison of the local Nusselt number (assuming negligible axial conduction) along the channel axis with the results of Yu and Ameel [10, 11] and Wibulswas [16] for T and H2 cases.

RESULTS AND DISCUSSION

A square channel with unit dimensionless wall thickness is considered in this analysis. One quarter of the channel is considered in the model due to symmetry. The value of β was taken as 0.6 (i.e. Pr=0.7 and γ=1.4) which is a reasonable assumption for gas flows. The effects of rarefaction and wall-conduction on the heat transfer in mirochannels with constant heat flux (H2) and constant wall temperature (T) thermal boundary conditions are examined for different values of Knudsen numbers and wall-fluid conduction ratios. Figure 4 shows the effect of rarefaction on the fully developed velocity profile. As Kn increases, the maximum velocity that occurs in the core region decreases while velocity slip at the wall increases.

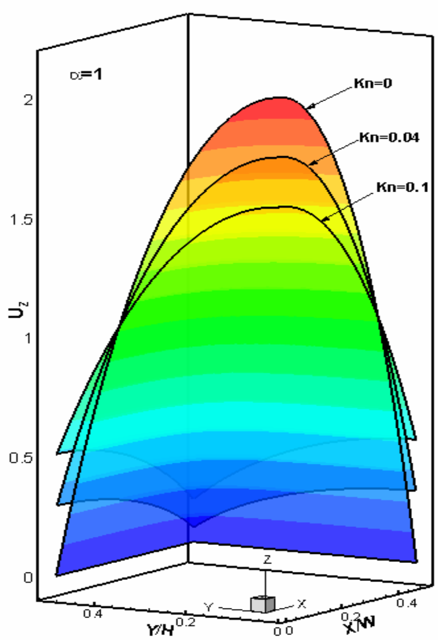

Fig. 4 Effect of Kn on the fully developed velocity profile for a square microchannel.

THEMALLY DEVELOPING TEMPERATURE FIELD

The effect of the Kn on the developing temperature profile is shown in Figs. 5(a) and 5(b) for a square microchannel with a conductive wall subjected to H2 and T thermal boundary conditions, respectively. As Kn increases, temperature profile deviates considerably that of no-slip flow case due to the presence of a large temperature jump at the wall-fluid interface.

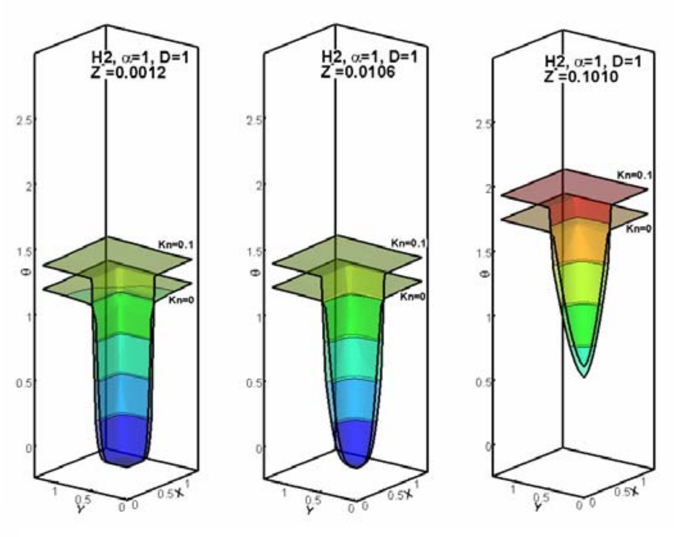

(a)

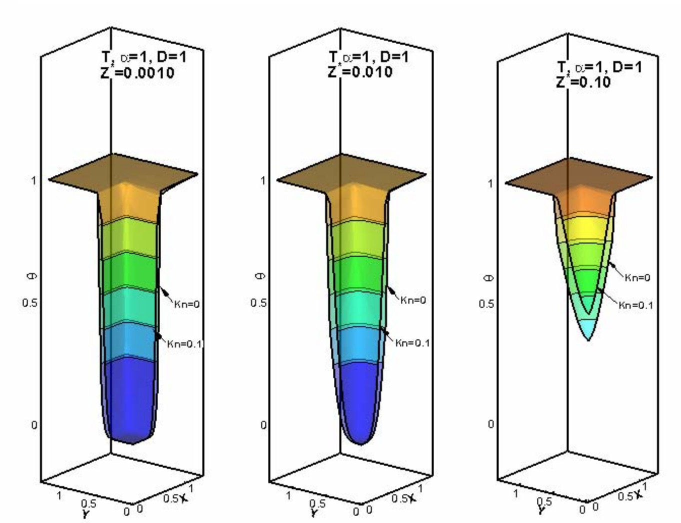

(b)

Fig. 5 Effect of rarefaction on the thermally developing temperature profile in a square channel with a conductive wall (d=1, conduction ratio k_s/k_f=200) at $Kn=0$ and 0.1 for (a) H2 and (b) T cases.

The effect of slip-flow and wall conduction on the average heat flux at the wall-fluid interface is shown in Fig. 6(a) for the H2 boundary condition. For the case of no wall conduction, the heat flux remains constant along the channel length. When the wall is included in the solution, the heat flux significantly increases at the beginning of the channel and then gradually decreased along the channel. This is due to the influence of heat conduction in the wall.

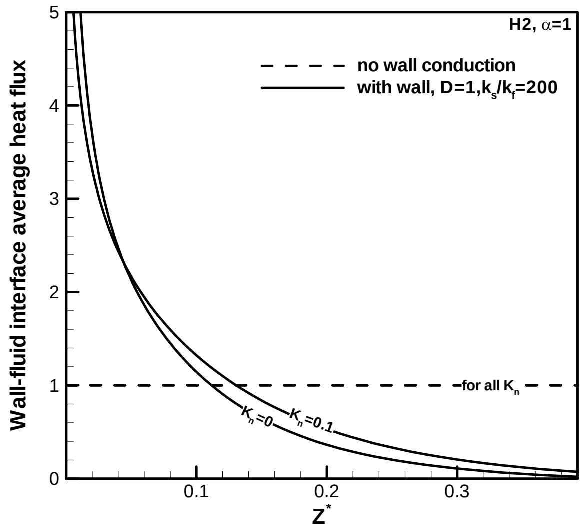

(a)

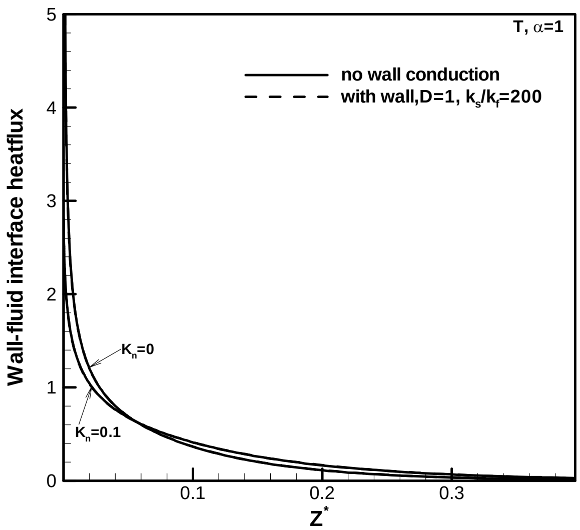

(b)

Fig. 6 Variation of the average wall-fluid interface heat flux along the channel length of a square microchannel with conductive wall for thermally developing flow at different *Kn* values. (a) H2 boundary condition. (b) T boundary condition.

The average fluid temperature for thermally developing flow with H2 and T thermal boundary conditions are shown in Figs 7(a) and 7(b). In the case of the H2 thermal boundary condition with no wall, the mean fluid temperature linearly increases along the channel axis. However, when the wall conduction is introduced, the average fluid temperature increases rapidly at the very beginning of the channel as shown in Fig. 7(a). This could be due the presence of a large heat flux in the beginning of the channel. In the case of the T thermal boundary condition, no obvious effect of wall conduction on wall-fluid interface heat flux and average fluid temperature is observed as shown in Figs 6(b) and 7(b). Average fluid temperature tends to decrease with the increase of Knudsen number in the thermally developing region for both H2 and T conditions with wall.

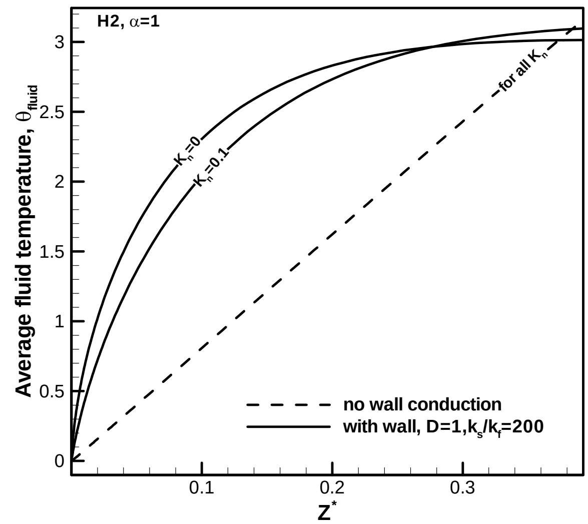

(a)

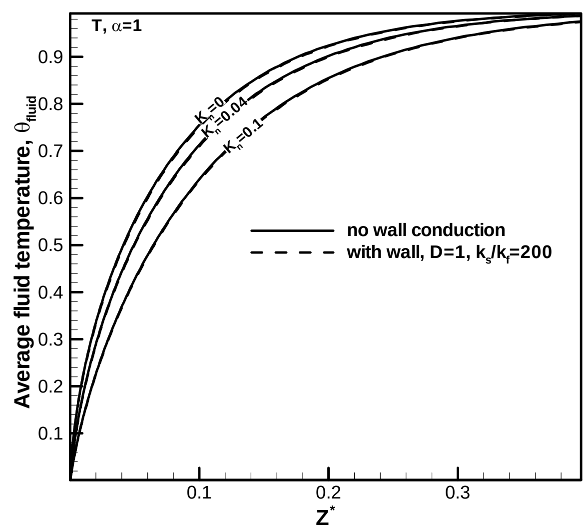

(b)

Fig. 7 Variation of average fluid temperature along the channel length of a square microchannel with conductive wall for thermally developing flow at different *Kn* values. (a) H2 boundary condition. (b) T boundary condition.

THERMALLY DEVELOPING NUSSELT NUMBER

The effect of *Kn* and wall conduction on the developing *Nu* along the axis of a square microchannel is shown in Figs. 8 and 9 for H2 and T thermal boundary conditions, respectively. The wall conduction has an increasing effect on the developing *Nu* number at the very beginning of the entrance region, particularly for no-slip flow and at small

Kn values, as shown in Fig. 8 for the case of the H2 thermal boundary condition. This could be due to fact that the presence of large heat flux at the wall-fluid interface in the very beginning of the entrance region as shown in Fig. 6(a). As the flow thermally develops, a slight decrease in Nu is observed towards the end of the entrance region, which could be due to the presence of weak wall-fluid interface heat flux. The wall conduction effect becomes less obvious at the very beginning of the entrance region for large *Kn* numbers as shown in Fig. 8(b). This could be due the presence of large temperature jump in the very begging of the entrance region due to the strong rarefaction effects.

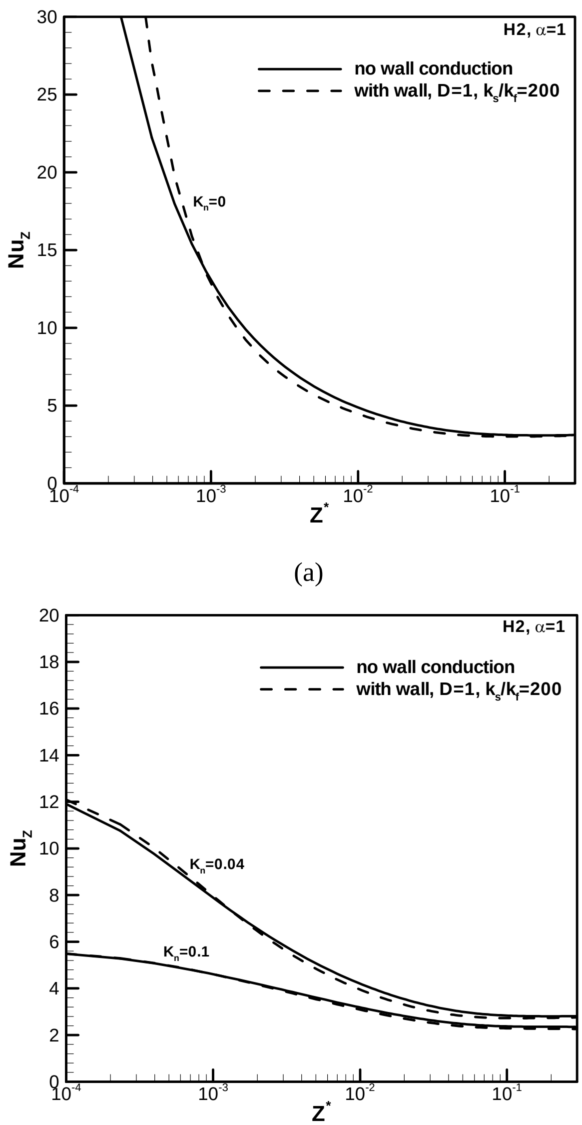

(a)

(b)

Fig. 8 Effect of rarefaction and wall conduction on the developing local Nusselt number along the axis of a square microchannel with H2 boundary condition at (a) *Kn=0* (b) *Kn=0.04* and *Kn=0.1*.

For the T thermal boundary condition, the effect of wall conduction has no significant effect on the slip-flow *Nu* number as shown in Fig. 9. This is due to the presence of uniform temperature in the wall that results in a negligible heat transfer along the axial direction of the channel wall.

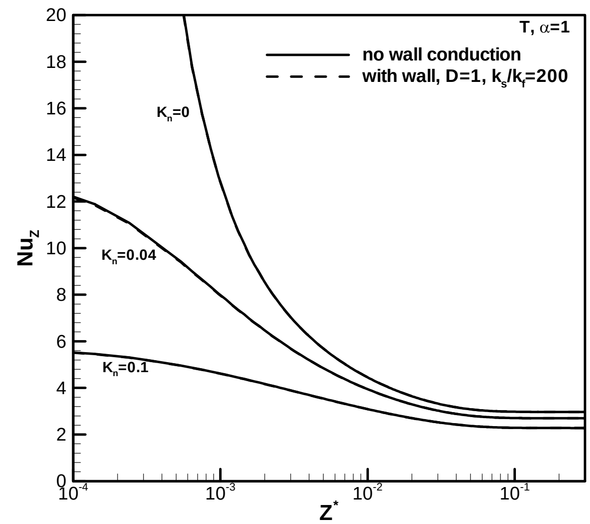

Fig. 9 Effect of rarefaction and wall conduction on the developing local Nusselt number along the axis of a square microchannel with T boundary condition at *Kn=0, Kn=0.04* and *Kn=0.1*.

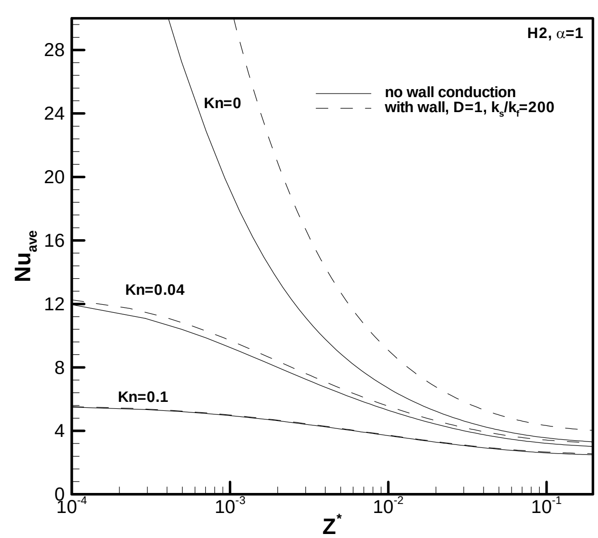

Fig.10 Effect of Knudsen number and wall conduction on the average Nusselt number along the axis of a square microchannel with H2 boundary condition

To better understand the effect of wall conduction and slip flow on the Nusselt number for the H2 thermal boundary condition, the average Nusselt number along the channel is plotted as shown in Fig. 10. A considerable increase in average Nu is observed in the case of no-slip flow case when the wall conduction is included. As slip increases, the effect of wall conduction on the Nu becomes less obvious.

CONCLUSIONS

The influence of conjugate heat transfer and slip-flow on the Nusselt number in rectangular microchannels is studied numerically for thermally developing laminar flow subjected to constant wall heat flux (H2) and constant wall temperature (T) boundary conditions. The coupled energy equations in the wall and fluid regions together with temperature jump at the boundary are solved using the finite volume method in a three-dimensional Cartesian coordinate system. A modified convection-diffusion coefficient at the wall-fluid interface is defined to incorporate the temperature-jump boundary condition. The effect of rarefaction and wall conduction on the heat transfer in the entrance region is analyzed in detail. Results show that the wall conduction has a considerable influence on the developing Nusselt number along the channel for the H2 boundary condition, particularly at low Knudsen numbers. In the case of the T boundary condition, no obvious influence of wall conduction on the Nusselt number is observed in the range of Knudsen numbers considered in this study.

REFERENCES

[1] E.G.R. Eckert, R.M. Drake, Jr., 1972, "Analysis of Heat and Mass Transfer", McGraw-Hill, New York, pp. 467–486.

[2] G. Karniadakis, A. Beskok, N. Aluru, 2005, "Microflows and Nanoflows: Fundamental and Simuation", Springer.

[3] W.A. Ebert, E.M. Sparrow, 1965, "Slip Flow in Rectangular and Annular Ducts", Journal of Basic Engineering, Transactions of the ASME, pp. 1018–1024.

[4] R.F. Barron, X. Wang, T.A. Ameel, R.O. Warrington, 1977, "The Graetz problem extended to slip-flow", International Journal of Heat and Mass Transfer, vol. 40, no. 8, pp. 1817–1823.

[5] T.A. Ameel, R.F. Barron, X. Wang, R.O. Warrington, 1977, "Laminar forced convection in a circular tube with constant heat flux and slip flow", Microscale Thermophysical Engineering, vol. 1, no.4, pp. 303–320.

[6] F.E. Larrodé, C. Housiadas,Y. Drossinos, 2000, "Slip-flow heat transfer in circular tubes", International Journal of Heat and Mass Transfer, vol. 43, pp. 2669–2680.

[7] Wei Sun, Sadik Kakac and Almila G. Yazicioglu, 2007, "A numerical study of single-phase convective heat transfer in microtubes for slip flow", International Journal of Thermal Sciences, vol. 50, no.17, pp. 3411-3421.

[8] Laxmidhar Biswal, S.K. Som, Suman Chakraborty, 2007, "Effects of entrance region transport processes on free convection slip flow in vertical microchannels with isothermally heated walls", International Journal of Heat and Mass Transfer, vol. 50, pp. 1248-1254.

[9] Nishanth Dongari, Abhishek Agrawal, Amit Agrawal, 2007, "Analytical solution of gaseous slip flow in long microchannels", International Journal of Heat and Mass Transfer, vol. 50, pp 3411-3421.

[10] S. Yu, T.A. Ameel, 2001, "Slip flow heat in rectangular microchannels", International Journal of Heat and Mass Transfer, vol. 44, pp 4225–4234.

[11] S. Yu, T.A. Ameel, 2002, "Slip-flow convection in isoflux rectangular microchannels", Journal of Heat Transfer, vol. 124, pp. 346–355.

[12] N.G. Hadjiconstantinou, O. Simek, 2002, "Constant-wall-temperature Nusselt number in micro and nano-channels", Journal of Heat Transfer, vol. 124, pp 356–364.

[13] M. Renksizbulut, H. Niazmand, G. Tercan, 2006, "Slip-flow and heat transfer in rectangular microchannels with constant wall temperature", International Journal of Thermal Sciences, vol. 45, no. 9, pp. 870-881.

[14] HD Madhawa Hettiarachchi, MN Golubovic, WJ Minkowycz, "Three dimensional slip flow heat transfer in a rectangular microchannel with constant wall temperature", International Journal of Heat and Mass Transfer (in press).

[15] S.V. Patankar, 1980, "Numerical Heat Transfer and Fluid Flow" , Hemisphere, Washington.

[16] P. Wibulswas, 1966, "Laminar Flow Heat Transfer in Noncircular Ducts", PhD thesis, London University, London.

